Research Article

Journal of Environmental Nanotechnology

A Study on the Photocatalytic and Antimicrobial Activities of Chitosan–ZnO Nanocomposites

K. Jothivenkatachalam[1*], A. Nithya[2] and S. Karthikeyan[3]

[1]Department of Chemistry, Anna University, BIT-campus, Tiruchirappalli, TN, India
[2]Department Of Energy Science, Alagappa University, Karaikudi, TN, India
[3]PG & Research Department of Chemistry, Chikkanna Government Arts College, Tirupur, TN, India
Received: 23.11.2023 Accepted: 05.12.2023 Published: 30-12-2023
*kjothivenkatachalam@gmail.com

ABSTRACT

ZnO nanoparticles can have their size, crystalline phase and aggregation inhibited by the biocompatible polymer chitosan. The production of ZnO nanoparticles with chitosan assistance was carried out using Sol-gel methodology. The nanoparticles have been studied using XRD, TGA, Surface analysis and HR-TEM. According to the findings, ZnO nanoparticles have a hexagonal shape and a particle size of roughly 91 nm. The synthesized nanoparticles exhibit improved photocatalytic activity for reactive dyes for Congo red when exposed to sunlight. The Langmuir-Hinshelwood (L-H) model revealed that the kinetics followed a pseudo-first-order. Additionally, the antibacterial activity was tested against the gram-negative *Escherichia coli* bacteria.

Keywords: ZnO; Chitosan; Photocatalytic degradation; Antimicrobial.

1. INTRODUCTION

Water pollution is a major problem due to the rapid development of science and technology, particularly in developing countries (Jothivenkatachalam *et al*. 2015; Giri *et al.* 2011). Large amounts of water are needed by many industries, including the chemical, petrochemical, pharmaceutical, textile and printing sectors. Huge amounts of wastewater are also released into the environment. Dye waste is a major hazardous pollution that cannot be broken down by nature, irreversibly damaging the ecology. Moreover, standard conventional procedures are inadequate for treating dye effluent due to the vast quantity of aromatic compounds and the stability of dye molecules (Lv *et al.* 2011; Suresh *et al.* 2013). Due to the production of active hydroxyl-free radical (•OH) as a primary byproduct of the irradiation of semiconductor materials, heterogeneous photocatalysis has been demonstrated to be a successful advanced oxidation technology for the full mineralization of hazardous organic compounds. Zinc oxide is a kind of wide band gap semiconductor (3.37 eV) having higher electron mobility as well as higher strength among the metal oxides (Xiao *et al.* 2014). The main advantage of ZnO lies in its appreciable good gas-sensing property, photocatalytic activity, antibacterial activity, optical property, low cost, etc. (Lv *et al*. 2011; Giri *et al*. 2011). The photocatalytic mechanism is mainly based on the formation of electron and hole pairs that are capable of removing organic dyes upon light illumination. Efforts have been made by many researchers to effectively increase the catalytic activities of semiconductors (Rajbongshi *et al*. 2015). The literature survey has shown that semiconductor-supported materials widely enhance photocatalytic activity because of their controllable pore space and surface chemistry, as well as photo stability (Suresh *et al.* 2013; Ambrozic *et al.* 2011). Congo red is an anionic azo dye and its IUPAC name is disodium 4-amino-3-[4-[4-(1-amino-4-sulfonato-naphthalen-2-yl) diazenylphenyl] phenyl] diazenyl-naphthalene-1-sulfonate.

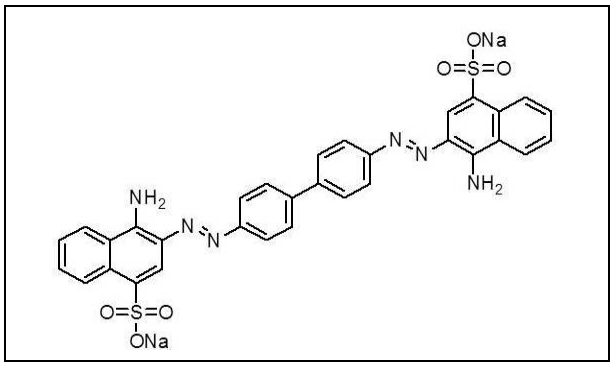

Fig. 1: Structure of Congo red

Congo red's molecular formula is $C_{32}H_{22}N_6Na_2O_6S_2$ with a molar mass of 696.66 g/mol, and its molecular structure is shown in Fig. 1. Congo red is water soluble, giving a red colloidal solution; its solubility is better in organic solvents. It has a strong affinity towards cellulose fibers (Gao *et al.* 2015). However, the use of Congo red in the cellulose industries such as cotton textile, wood pulp and paper has long been

abandoned, primarily because of its toxicity and metachromatic property. Chitosan (CS) is an interesting biopolymer for immobilization due to its excellent film-forming ability, high permeability, good mechanical strength, nontoxicity, biocompatibility, low cost and easy availability (Jayaseelan *et al*. 2012; Han *et al.* 2015; Zhang *et al.* 2007). The binding ability of chitosan was attributed to the chelating groups such as $–NH_2$ and –OH with metal. The different chitosan composite materials such as Chitosan/TiO_2 (Yang *et al*. 2014; Han *et al.* 2015; Gao *et al.* 2015; Rajbongshi *et al*. 2014; Marschall *et al.* 2013; Zhang *et al.* 2007; Rajbongshi et al. 2015; Ali *et al.* 2012), Chitosan/Cuprous oxide (Chen *et al*. 2008), Chitosan/CdS (Xu *et al.* 1997) and Chitosan/ZnO (Xu *et al.* 1997; Chatti *et al.* 2007; Lin *et al.* 2014; Jothivenkatachalam *et al.* 2014; Nithya *et al*. 2014; Sudheesh *et al.* 2012; Zainal *et al*. 2009; Nawi *et al.* 2010) were prepared for the application of antibacterial agent, biosensor and photocatalyst to remove organic pollutants. The present investigation deals with the synthesis of Zinc oxide nanoparticles using a Chitosan biopolymer, its characterization and application on photocatalysts and antibacterial activity. The photocatalytic experiment on the degradation of Rhodamine B (RhB) and Methyl orange (MO) was carried out under irradiation of solar and visible light. Antibacterial activity for the nanoparticles was performed using the gram-negative Escherichia coli bacteria (Ru *et al.* 2009).

2. EXPERIMENTAL METHODS

2.1 Materials

Zinc acetate dihydrate, tungstic acid, chitosan, glacial acetic acid, sodium hydroxide, glacial acetic acid and sodium chloride used were of analytical grade. All the solutions were prepared with double distilled water. Congo red (anionic dye, MW=696.66 g/mol) of analytical grade was used for photocatalytic reaction. Nutrient Agar (NA) and Mueller–Hinton Agar (MHA) for the cultivation of bacteria were obtained from Hi-media, India. Standard microbial strains of *E. coli (*MTCC 1687) were procured from the Institute of Microbial Technology, Chandigarh, India.

2.2 Synthesis

The ZnO was prepared by Sol-gel method using zinc acetate and sodium hydroxide precursors. 50 ml of 0.12 M Zinc acetate was added into 50 ml of 0.5 M sodium hydroxide solution under constant stirring at room temperature for 2 h. The obtained white precipitate was centrifuged and washed several times with water to remove unreacted precursors and then dried at 80 $^{\circ}$C for 5 h. Chitosan-ZnO (CS-ZnO) nanocomposite was prepared by mixing 20 ml of 1 % chitosan in 0.1 M of CH_3COOH and 8 ml (0.2 M) NaCl and stirring continuously overnight to dissolve the chitosan. As-prepared ZnO (0.2 M) was kept in contact with the viscous solution and stirred continuously for about 24 h at 700 rpm. Then, the mixture was centrifuged and the supernatant was separated. The solid residue was filtered and washed several times with water to avoid excess acetic acid, and then dried at 80 $^{\circ}$C for 5 hrs.

2.3 Characterization

Powder XRD data was collected *via* Philips PW 1710 Diffractometer with Cu-Kα radiation (k = 1.5406 A$^{\circ}$) and graphite monochromator, operated at 45 kV; 30 mA and 25 $^{\circ}$C. The amount of free water was determined by TGA, which was performed on a Mettler TA 3000 Thermal analyzer under a nitrogen atmosphere at a heating rate of 5 $^{\circ}$C min^{-1} with a sample weight of 3–5 mg. DSC measurements were performed on a Mettler Toledo STARe system to scan the synthesized material under a dry nitrogen atmosphere in an unsealed alumina pan. The size and shape of the nanocomposites were analyzed using TECNAI T20 HRTEM operating at 200 keV and the phase analysis was done by observing the SAED pattern. The Photocatalytic experiments were carried out in the photo reactor Heber Visible Annular Type Photo reactor equipped with a 300 W tungsten halogen lamp (8500 lm). The antimicrobial potential of the synthesized nanocomposite was tested against standard microbial strains.

2.4 Photocatalytic Activity

Photocatalytic experiments were carried out in the Heber Visible Annular Type Photo reactor equipped with a 300 W Tungsten Halogen lamp (8500 lumens). The solution was illuminated with a light source at the center of the solution reservoir, covered and separated by cylindrical quartz glass housing. Air was bubbled through the reaction solution to ensure a constant supply of oxygen and to give an agitation effect to achieve the equilibrium state of the model pollutant and photocatalyst. At given irradiation time interval, an aliquot amount of the samples was taken and analyzed by UV-Visible spectrometer at the wavelength of maximum absorbance for CR (k_{max} = 497 nm).

2.5 Antibacterial Activity

The antimicrobial activity of as-prepared ZnO and ZnO (CS) were tested against gram-negative bacteria *E. coli* (ATCC 8739). The test samples were prepared by dispersing them in sterile distilled water using an ultrasonicator. Standard antibiotic streptomycin was used as positive control and sterile distilled water as negative control. Well diffusion technique was followed to perform the antimicrobial test for which freshly grown cultures were used as inoculums in an NA medium. Approximately 20 ml of NA medium was poured into sterilized Petri dishes. The plates were left overnight at room temperature to check for contamination. The test

organisms were grown in selected broth for 24 h. Wells of 5 mm diameter were made on NA plates and were gel-punctured using sterile pipette tips. Using a micro-pipette, 20 ml was poured into the wells. After incubation at 37 °C for 24 h, the different levels of zone of inhibition of bacteria were measured.

3. RESULTS AND DISCUSSION

3.1 Powder XRD

The XRD pattern of CS-ZnO nanoparticles was shown in Fig. 2. The peaks appeared with 2θ values of 31.8°, 34.5°, 36.4°,47.6°, 56.5°, 63°, 66.5°, 68.1° and 69.1° corresponds to (100), (002), (101), (102), (110), (103), (200), (112) and (201) crystal planes of hexagonal geometry, and the lattice parameters were determined to be a = 3.2420 and c = 5.1845 that matches with the JCPDS file no. 79-2205. The average crystalline size, calculated by Debye Scherrer's equation, was 48 nm; the sharp peak of XRD pattern revealed that there is no impurity present in the sample and the structure was highly crystalline.

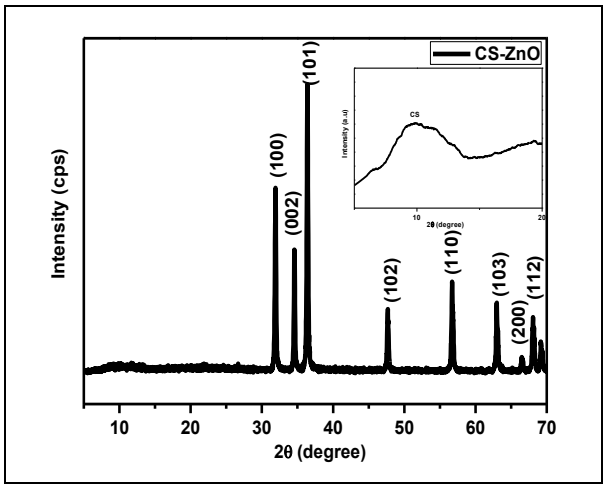

Fig. 2: XRD pattern of CS-ZnO nanocomposite

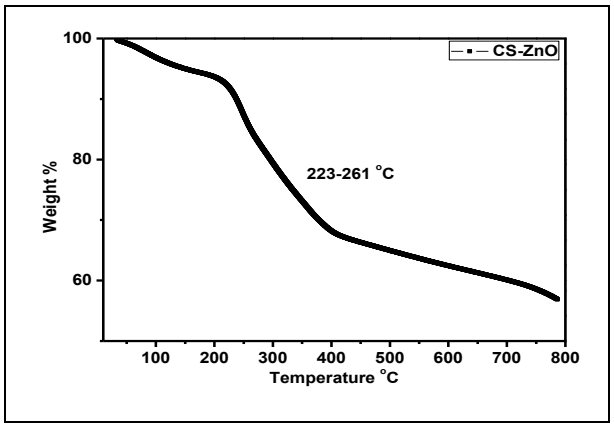

Fig. 3: TGA analysis of CS-ZnO nanocomposite

3.2 Thermal Analysis

TGA analysis of CS-ZnO nanocomposite result is presented in Fig. 3. Four weight losses were observed. Weight loss of 5% was observed at 62.78-112.64 °C, 13% of weight loss at 223.98-261.85 °C, 11% of weight loss at 261.85-359.73 °C and then 9% of weight loss at 359.73-397.99 °C. The weight loss around 100 °C was due to moisture vaporization and the loss up to 397.99 °C was due to the degradation of CS in the nanocomposite. The total weight loss of CS-ZnO nanocomposite was about 43.11% at 800 °C. Therefore, it can be concluded that CS-ZnO shows better thermal stability than pure chitosan due to the presence of ZnO in the nanocomposite.

3.3 Surface Area and Surface Charge Analysis

The N_2 adsorption-desorption isotherms were measured using N_2 Adsorption-Desorption Analyzer. CS-ZnO nanocomposite shows a type IV isotherm indicating the formation of micropores and the hysteresis loops were observed in Fig. 4. Surface area was calculated by multiple BET analysis and was found to be 32.4 m^2g^{-1}. The total pore volume obtained at P/P_o was 0.1808 ccg^{-1} and the pore size was 18 nm, as calculated by BJH method. Surface charge of CS-ZnO nanocomposite was analyzed for the stability of nanocomposite. The zeta potential analysis is shown in Fig. 5 and was found to be -2.0 mV.

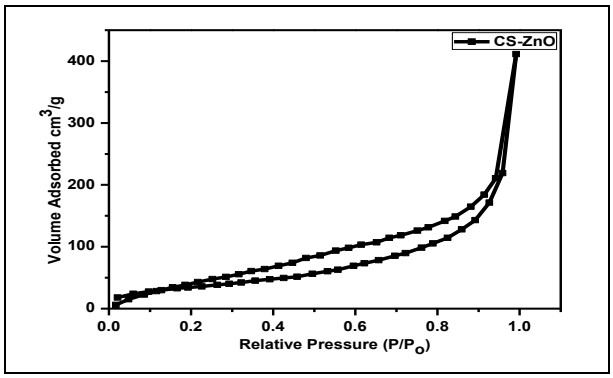

Fig. 4: N_2 adsorption-desorption isotherm of CS-ZnO nanocomposite

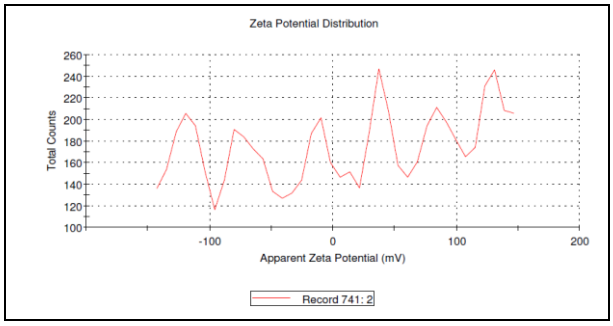

Fig. 4: Zeta potential analysis of CS-ZnO nanocomposite

3.4 HR-TEM

HR-TEM image implies the presence of hexagonal nano-structured particles of length 475 nm and width 234 nm, as shown in Fig. 6 (a). The dark spots observed in the SAED pattern were shown in Fig. 6 (b), which can be indexed to be hexagonal structures.

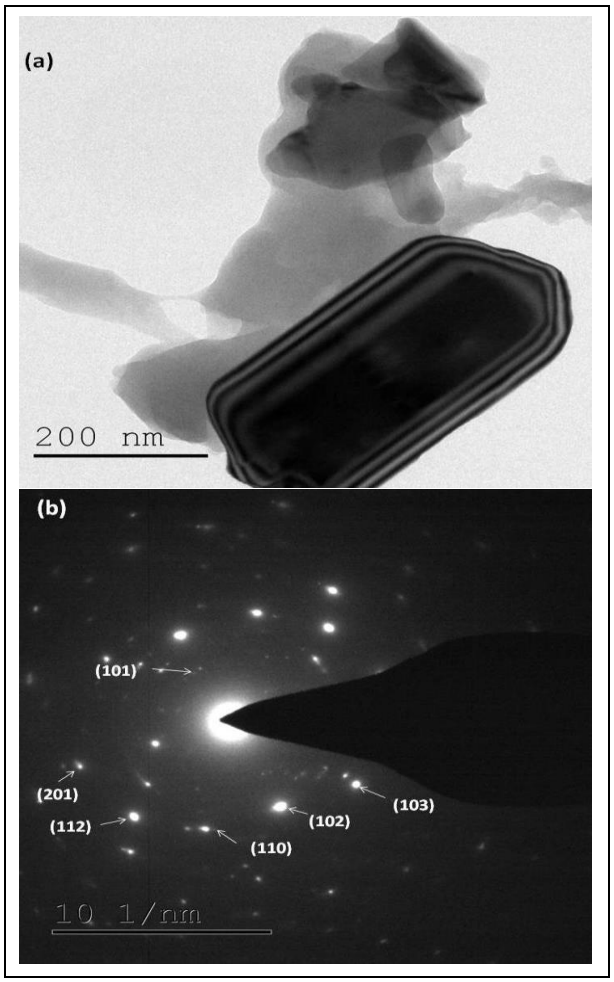

Fig. 6: (a) HR-TEM image and (b) SAED pattern of CS-ZnO nanocomposite

3.5. Photocatalytic Activity

The potential application of CS-ZnO nanoparticles towards the treatment of dye in wastewater can be done by heterogeneous photocatalysis route. In this present study, reactive dyes of Congo red (CR) were considered as a pollutant. The effect of photocatalysts on the removal of dyes was monitored by the changes in the absorption spectrum of the respective dye in different time scales. To study the activity of the catalyst, control experiments for CR were done under visible light irradiation for 180 min. No considerable change was observed in the absorption spectra of dye molecules, indicating that the dye molecules remained stable during the reaction time.

3.6 Effect of Catalyst Amount

The photocatalytic activity was again carried out for a Congo red dye. Likewise, the aqueous solution of CR (5.74168 x 10^{-5} M) dyes were subjected to photocatalytic studies and the amount of catalyst was taken in the range from 0.1 to 0.4 gL^{-1}. The UV-Vis absorption spectrum of CR has shown that the maximum absorbance occurred at 494 nm which is λ_{max} for CR dyes. Among the various amounts of catalyst from 0.1 to 0.4 gL^{-1}, 0.3 gL^{-1} has shown 97% decolorization for CR dyes under visible light irradiation. However, when the amount of catalyst was increased beyond the limit of 0.3 gL^{-1}, the photocatalytic activity decreased owing to the inner filter effect. The increase in the catalyst amount beyond the limit did not have a noticeable positive effect on the decolorization of reactive dyes because of the enhancement of light reflectance and light blocking by excessive catalyst and decrease in light penetration. The kinetic plot of ln (C_o/C) *vs* irradiation time under visible light illumination is presented in Fig. 7 (a). The higher rate constant (k) value of 0.01471 min^{-1} was obtained for 0.3 gL^{-1} concentration of catalyst for CR dye. The correlation coefficient value (R^2) was found to be greater than 0.95, which showed that all the values were highly significant and also confirmed the proposed kinetic model for the decolorization of reactive dyes. The corresponding absorption spectrum for decolorization of CR dyes under visible light irradiation is shown in Fig. 7 (b).

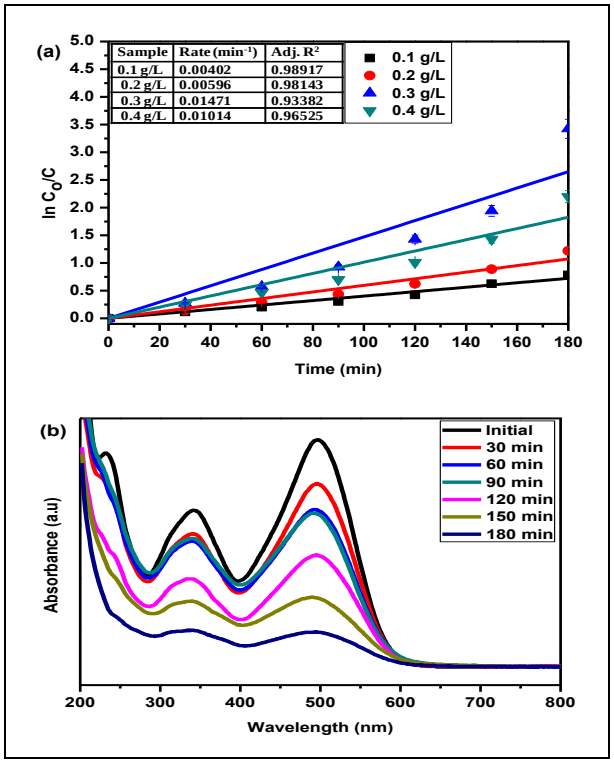

Fig. 7: (a) Kinetic plot of ln (C_o/C) Vs Irradiation time of CS-ZnO nanocomposite at catalyst concentration variation under visible light irradiation for CR dye and (b) Time dependent absorption spectra of CR dye at 0.3 gL^{-1} of CS- ZnO nanocomposite under visible light irradiation

3.7 Effect of pH

The pH of the dye solution plays a predominant role in the decolorization of dyes, it determines the electrostatic interaction of the surface charge of the catalyst with the dye molecules. The dye concentrations of RhB (1.04 x 10^{-5} M), MO (3.05502 x 10^{-5} M) and CR (5.7416 x 10^{-5} M) and the catalyst concentration of 0.3 g L^{-1} were used to study the effect of pH by varying from 3 to 11. The pH of the solution was adjusted with the help of HCl or NaOH by measuring using the pH meter. The kinetic plot for CR for pH variations was presented in Fig. 7. The rate constant values obtained from the slope of the plots were tabulated at the insets of Fig. 8. The greater degradation rate of 0.00399 min^{-1} was monitored at a basic pH for CR dye. In the case of CR, at acidic pH 3.0, the colour of the dye solution changed to blue and the λ_{max} also shifted to 577 nm which showed that CR molecules possessed aggregation in an acidic aqueous solution.

3.8 Adsorption Study

The adsorption study of CR dyes on the surface of CS-ZnO nanocomposite was carried out under dark conditions. CR dye concentration of 5.7416 x 10^{-5} M and the optimized catalyst concentration of 0.3 gL^{-1} were used. The decrease in absorption peak was mainly due to the powerful adsorption capability of CS-ZnO nanocomposite. The adsorption percentage towards CR dyes was 40%.

3.9 Antimicrobial Activity

The antimicrobial activity of the synthesized CS-ZnO nanocomposite was tested against five standard strains comprising of two gram-positive bacteria (*Staphylococcus aureus*, MTCC 96 and *Streptococcus pneumonia*, MTCC 1936), two gram-negative bacteria (*Pseudomonas aeruginosa*, MTCC 2642 and *Proteus vulgaris*, MTCC 7299), and one fungal (*Candida albicans*, MTCC 3959). The synthesized CS-ZnO nanocomposite showed antimicrobial activity against standard microbes, as depicted in Fig. 9 and Fig. 10. The zone of inhibition for gram-positive and gram-negative bacteria and fungal pathogens were represented as a bar diagram in Fig. 11. The antimicrobial activity of CS-ZnO nanocomposite increased with the increase of concentration from 10 to 100 µg. The CS-ZnO nanocomposite with 100 µg of concentration showed the maximum zone of inhibition ranging between 2.66667 ± 0.57735 and 25±1 (mm). The positive results were observed for both gram-positive and gram-negative bacteria with *S. aureus* - 17.66667± 0.57735 (mm), *S. Pneumoniae* - 25±1 and *P. vulgaris* - 20.66667± 0.5773 (mm). The fungal *C. albicans* did not show activity at a lower concentration, but it posed 3 ± 1 (mm) at 100 µg of CS-ZnO nanocomposite.

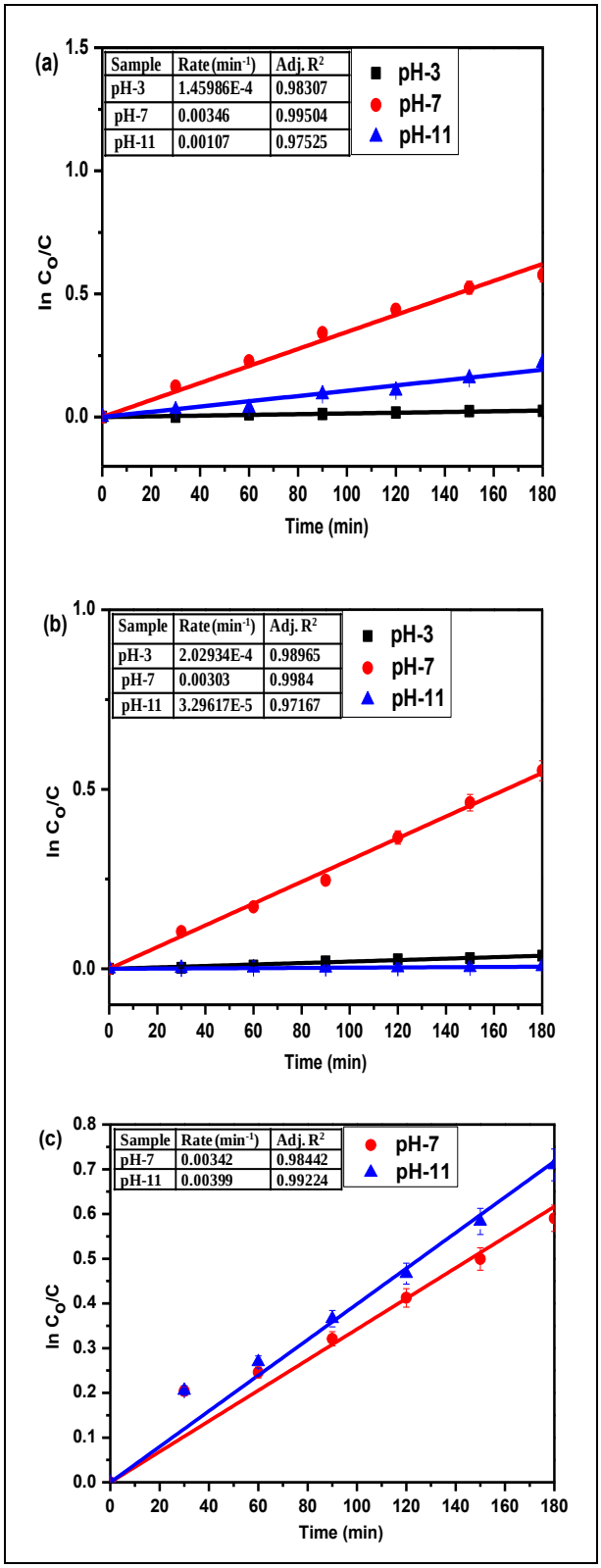

Fig. 8: Kinetic plot of ln (C_o/C) Vs irradiation time of CS- ZnO nanocomposite at pH variation under visible light irradiation for CR dye

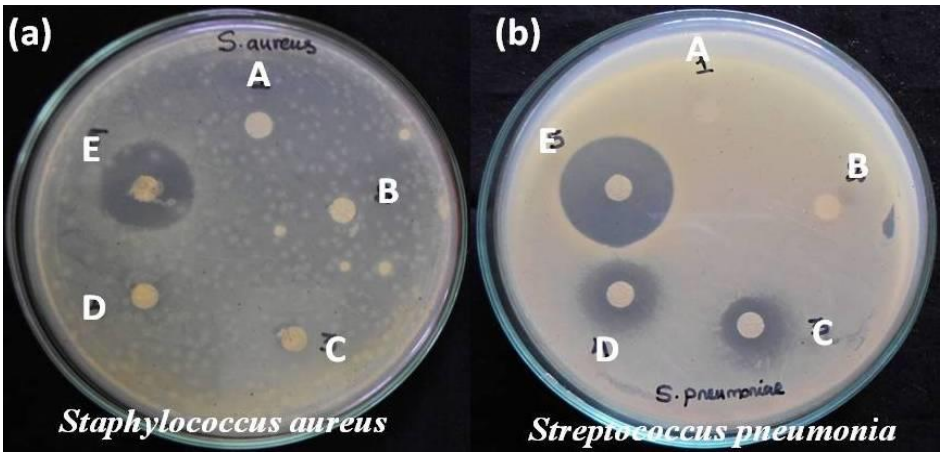

Fig. 9: Antimicrobial activity of CS-ZnO nanocomposite against gram-positive bacterium (a) *Staphylococcus aureus* (MTCC 96) and (b) *Streptococcus pneumonia* (MTCC 1936)– (A) Distilled Water 100 µL, (B) Chitosan 10 µg, (C) CS-ZnO nanocomposite 10 µg, CS-ZnO nanocomposite 50 µg and (D) CS-ZnO nanocomposite 100 µg

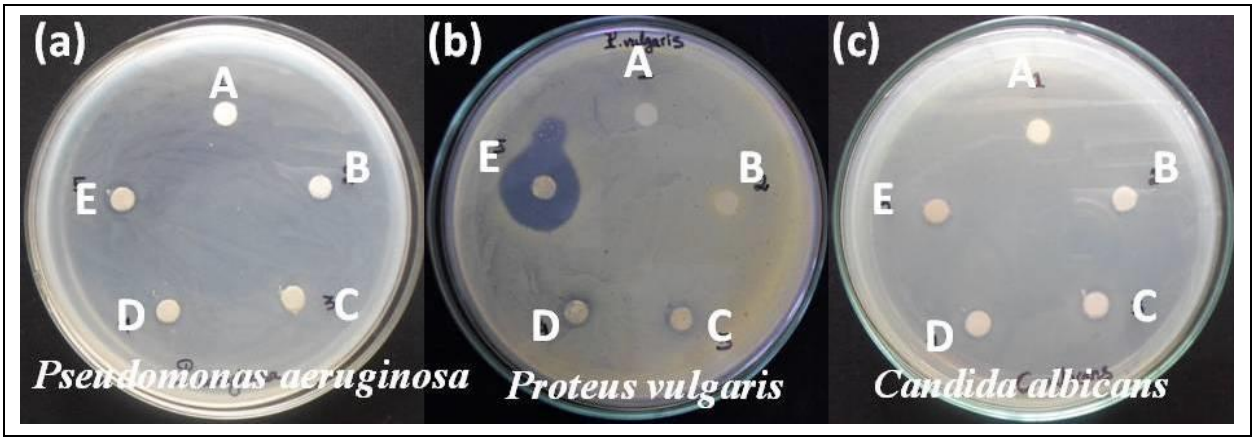

Fig. 10: Antimicrobial activity of CS-ZnO nanocomposite against gram-negative bacterium (a) *Pseudomonas aeruginosa* (MTCC 2642), (b) *Proteus vulgaris* (MTCC 7299) and (c) Fungal *Candida albicans (MTCC 3959)* – (A) Distilled Water 100 µL, (B) Chitosan 10 µg, (C) CS-ZnO nanocomposite 10 µg, CS-ZnO nanocomposite 50 µg and (D) CS-ZnO nanocomposite 100 µg

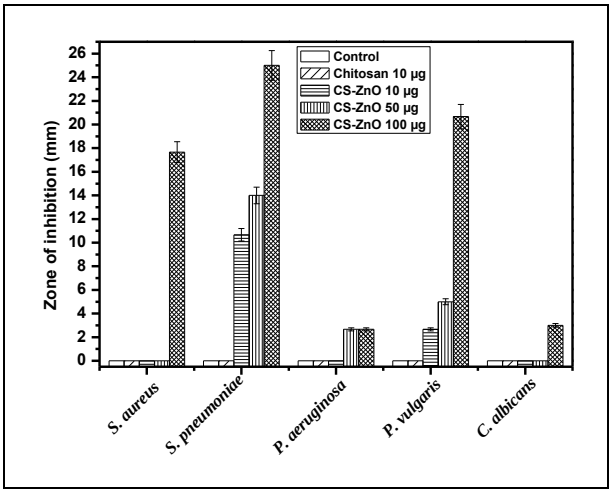

Fig. 11: Antimicrobial activity of CS-ZnO nanocomposite

4. CONCLUSION

The ZnO nanoparticles were synthesized using a biopolymerand characterized by analytical techniques. The band gap of ZnO (CS) was calculated using reflectance spectra and was found to be 3.1 eV, which was less than the band gap of as-prepared ZnO. CS-ZnO showed better thermal stability than pure chitosan due to the presence of ZnO in the nanocomposite. The N_2 adsorption-desorption isotherms were measured using N_2 adsorption-desorption analyzer and the Zeta potential analysis was also done. The results revealed that the ZnO (CS) has a potential application in the decolorization of CR dyes. Studies on heterogeneous photocatalysis with the use of natural sunlight are rare, probably due to the variation in the solar irradiance, and hence it was reported that the effective decolorization of reactive dyes takes place by ZnO (CS) nanoparticles under the

utilization of natural sunlight. The decolorization experiment followed a pseudo-first-order rate constant using the L–H model and the correlation coefficient values were highly significant. The photocatalytic activity showed that the decolorization was much faster in solar light than in visible light and also exhibited enhanced antibacterial activity against the gram-negative *E. coli* bacteria.

FUNDING

This research received no specific grant from any funding agency in the public, commercial or not-for-profit sectors.

CONFLICTS OF INTEREST

The authors declare that there is no conflict of interest.

COPYRIGHT

This article is an open-access article distributed under the terms and conditions of the Creative Commons Attribution (CC BY) license (http://creativecommons.org/licenses/by/4.0/).

REFERENCES

Ali, A. M., Muhammad, A., Shafeeq, A., Asghar, H. M. A., Hussain, S. N. and Sattar, H., Doped Metal Oxide (ZnO) and Photocatalysis: a review, *J. Pak. Inst. Chem. Eng.*, 40(1), 11–19 (2012).

Ambrozic, G., Orel, Z. C. and Zigon, M., Microwave-assisted non- aqueous synthesis of ZnO nanoparticles, *Mater. Technol.*, 45(3), 173–177 (2011).

Chatti, R., Rayalu, S. S., Dubey, N., Labhsetwar, N., Devotta, S., Solar-based photoreduction of methyl orange using zeolite sup- ported photocatalytic materials, *Sol. Energy Mater. Sol. Cells*, 91(2), 180–190 (2007). http://dx.doi.org/10.1016/j.solmat.2006.08.009

Chen, J. Y., Zhou, P. J., Li, J. L. and Wang, Y., Studies on the photo- catalytic performance of cuprous oxide/chitosan nanocomposites activated by visible light, *Carbohydr. Polym.*, 72(1), 128–132 (2008). https://doi.org/10.1016/j.carbpol.2007.07.036

Chen, K. J., Fang, T. H., Hung, F. Y., Ji, L. W., Chang, S. J., Young, S. J., Hsiao, Y. J., The crystallization and physical properties of Al-doped ZnO nanoparticles, *Appl. Surf. Sci.*, 254(18), 5791–5795 (2008). https://doi.org/10.1016/j.apsusc.2008.03.080

Giri, P. K., Bhattacharyya, S., Chetia, B., Kumari, S., Singh, D. K. and Iyer, P. K., High-yield chemical synthesis of hexagonal ZnO nanoparticles and nanorods with excellent optical properties, *J. Nanosci. Nanotechnol.*, 12(1), 201–6 (2011). https://doi.org/10.1166/jnn.2012.5113

Han, D., Cao, J., Yang, S., Yang, J., Wang, B., Liu, Q., Wang, T. and Niu, H., Fabrication of ZnO nanorods/Fe3O4 quantum dots nanocomposites and their solar light photocatalytic performance. J. Mater, *Sci. Mater. Electron.*, 26, 7415–7420 (2015). https://doi.org/10.1007/s10854-015-3372-x

Jayaseelan, C., Abdul, R. A., Vishnu, K. A., Marimuthu, S., Santhoshkumar, T., Bagavan, A., Gaurav, K., Karthik, L. and Bhaskara, R. K. V., Novel microbial route to synthesize ZnO nanoparticles using Aeromonas hydrophila and their activity against pathogenic bacteria and fungi, *Spectrochim. Acta Part A.*, 90, 78–84 (2012). https://doi.org/10.1016/j.saa.2012.01.006

Jothivenkatachalam, K., Prabhu, S., Nithya, A. and Jeganathan, K., Facile synthesis of WO3 with reduced particle size on zeolite and enhanced photocatalytic activity, *RSC Adv.*, 4(41), 21221–21229 (2014). https://doi.org/10.1039/C4RA01376J

Jothivenkatachalam, K., Prabhu, S., Nithya, A., Chandra M. S. and Jeganathan, K., Solar, visible and UV light photocatalytic activity of $CoWO_4$ for the decolourisation of methyl orange, *Desalin. Water Treat.*, 54(11), 3134–3145 (2015). https://doi.org/10.1080/19443994.2014.906324

Lin, S. T., Thirumavalavan, M., Jiang, T. Y., Lee, J. F., Synthesis of ZnO/Zn nano photocatalyst using modified polysaccharides for photodegradation of dyes, *Carbohydr. Polym.*, 105, 1-9 (2014). https://doi.org/10.1016/j.carbpol.2014.01.017

Lv, J., Gong, W., Huang, K., Zhu, J., Meng, F., Song, X. and Sun, Z., Effect of annealing temperature on photocatalytic activity of ZnO thin films prepared by sol–gel method, *Superlattices Microstruct.*, 50(2), 98–106 (2011). https://doi.org/10.1016/j.spmi.2011.05.003

Marschall, R. and Wang, L., Non-metal doping of transition metal oxides for visible-lightphotocatalysis, *Catal. Today*, 225, 111-135 (2013). https://doi.org/10.1016/j.cattod.2013.10.088

Nawi, M. A., Sabar, S., Jawad, A. H., Sheilatina and Wan, N. W. S., Adsorption of Reactive Red 4 by immobilized chitosan on glass plates: towards the design of immobilized TiO2–chitosan syner- gistic photocatalyst-adsorption bilayer system, *Biochem. Eng. J.*, 49(3), 317–325 (2010). https://doi.org/10.1016/j.bej.2010.01.006

Nithya, A., Jothivenkatachalam, K., Prabhu, S., Jeganathan, K., Chitosan based nanocomposite materials as photocatalyst—a review, *Mater. Sci. Forum*, 781, 79–94 (2014). https://doi.org/10.4028/www.scientific.net/MSF.781.79

Rajbongshi, B. M., Ramchiary, A., Jha, B. M. and Samdarshi, S. K., Synthesis and characterization of plasmonic visible active Ag/ ZnO Photocatalyst, *J. Mater. Sci. Mater. Electron.*, 25, 2969–2973 (2014). https://doi.org/10.1007/s10854-014-1968-1

Rajbongshi, B. M., Samdarshi, S. K. and Boro, B., Multiphasic bi- component TiO2–ZnO nanocomposite: synthesis, characteriza- tion and investigation of photocatalytic activity under different wavelengths of light irradiation, *J. Mater. Sci.: Mater. Electron.*, 26, 377–384 (2015). https://doi.org/10.1007/s10854-014-2410-4

Ru, J., Huayue, Z., Xiaodong, L., and Ling, X., Visible light photocat- alytic decolourization of C. I. Acid Red 66 by chitosan capped CdS composite nanoparticles, *Chem. Eng. J.*, 152(2), 537–542 (2009). https://doi.org/10.1016/j.cej.2009.05.037

Sudheesh, K. P. T., Lakshmanan, V., Anilkumar, T. V., Ramya, C., Reshmi, P., Unnikrishnan, A. G., Nair, S. V. and Jayakumar, R., Flexible and microporous chitosan hydrogel/nano ZnO composite bandages for wound dressing: in vitro and in vivo evaluation, *Appl. Mater. Interfaces*, 4(5), 2618–2629 (2012). https://doi.org/10.1021/am300292v

Suresh, B. K. and Narayanan, V., Hydrothermal synthesis of hydrated zinc oxide nanoparticles and its characterization, *Chem. Sci. Trans.*, 2(1), 33-36 (2013). https://doi.org/10.7598/cst2013.004

Xiao, S., Liu, L., Lian, J., Solvothermal synthesis of nanocrystalline ZnO with excellent photocatalytic performance, *J. Mater. Sci. Mater. Electron*., 25, 5518–5523 (2014). https://doi.org/10.1007/s10854-014-2338-8

Xu, Y. and Langford, C. H., Photoactivity of titanium dioxide sup- ported on MCM41, zeolite X, and zeolite Y, *J. Phys. Chem. B*, 101, 3115–3121 (1997). https://doi.org/10.1021/jp962494l

Yang, J., Wang, X., Jiang, T., Li, Y., Ma, Q., Han, J., Chen, J., Wang, J. and Wang, Y., Controllable preparation, growth mechanism and the properties research of ZnO nanocrystal, *Superlattices Microstruct*., 72, 91-101 (2014). https://doi.org/10.1016/j.spmi.2014.04.006

Zainal, Z., Hui, L. K., Hussein, M. Z., Abdullah, A. H. and Hamad-neh, I. R., Characterization of TiO2–Chitosan/Glass photocatalyst for the removal of a monoazo dye via photodegradation–adsorption process, *J. Hazard. Mater*., 164(1), 138–145 (2009). https://doi.org/10.1016/j.jhazmat.2008.07.154

Zhang, Q., Fan, W., Gao, L., Anatase TiO2 nanoparticles immo- bilized on ZnO tetrapods as a highly efficient and easily recy- clable photocatalyst, *Appl. Catal. B*, 76, 168–173 (2007). https://doi.org/10.1016/j.apcatb.2007.05.024

Zhao, L., Efficient photocatalyst based on ZnO nanorod arrays/p- type boron-doped-diamond heterojunction. J. Mater. Sci.: Mater. Electron. 26, 1018–1022 (2015).